The Radiation Induced Order-Disorder Transformation in Cu_3Au

R. Zee and P. Wilkes

September 1979

UWFDM-314

FUSION TECHNOLOGY INSTITUTE

UNIVERSITY OF WISCONSIN

MADISON WISCONSIN

The Radiation Induced Order-Disorder Transformation in Cu_3Au

R. Zee and P. Wilkes

Fusion Technology Institute
University of Wisconsin
1500 Engineering Drive
Madison, WI 53706

http://fti.neep.wisc.edu

September 1979

UWFDM-314

The Radiation Induced Order-Disorder Transformation in Cu_3Au

R. Zee and P. Wilkes

September 1979

UWFDM-314

Fusion Engineering Program
Nuclear Engineering Department
University of Wisconsin
Madison, Wisconsin 53706

Published in Philosophical Magazine A 42 (1980) 463-482.

The Radiation Induced Order-Disorder Transformation in Cu_3Au

R. Zee and P. Wilkes

Abstract

A model for ordered alloys is presented which describes the combined effects of radiation disordering and radiation enhanced ordering. The model uses the assumptions of Bragg-Williams ordering in a kinetic form in which the ordering energy is a linear function of order. Point defect concentrations are introduced into the ordering kinetics so that the effect of the radiation (through enhancement of such concentrations) can be described. Both time dependent and steady-state solutions to the resulting ordering rate equation are presented.

All the available data on irradiation of Cu_3Au with fast and thermal neutrons are reviewed and presented as functions of long range order parameter (S) versus dose. All the curves at a wide variety of temperatures are fitted successfully with the model using the same diffusion parameters throughout. The implications and predictions of the model for future experiments are discussed.

The Radiation Induced Order-Disorder Transformation in Cu_3Au

R. Zee and P. Wilkes

University of Wisconsin-Madison

1. Introduction

Experiments have shown[1,2] that under irradiation previously stable alloys may undergo phase transformations. Second phase particles may dissolve or new ones form. One mechanism that has been proposed to explain phase dissolution is radiation disordering.[3] It has been demonstrated that the free energy change involved in this process is often comparable to the free energy of formation of alternative phases and irradiation modified phase diagrams have been calculated on this basis.[3] The process of radiation disordering has long been known to occur and has recently been reviewed.[3,4] However, enhanced radiation ordering is also a common observation so that the situation is evidently not simple. A model which permits calculation of both ordering and disordering rates under irradiation has recently been proposed[3] and it is the purpose of this paper to apply this model to all the available data on irradiation of Cu_3Au. This has been irradiated more than any other ordered alloy in the literature and good thermal ordering data is also available.

We demonstrate in this paper that all the available data can be satisfactorily fitted with this model, using the same parameters for the diffusional behavior of the alloy throughout.

2. The Radiation Disorder Model

When an energetic particle interacts with the lattice atoms of a metal to produce a cascade of displacements, it is well known that many

point defects are produced. In the process many more atoms can change position (replacements) than are displaced to produce Frenkel defects. In an ordered alloy such replacements produce disorder. This disorder has been used to make cascade regions visible in the electron microscope.[5]

In addition to these local cascade replacements, replacement collision sequences can also produce disorder. This occurs when a chain of atoms is displaced forward leaving a vacancy behind and an interstitial at the forward end. Since each atom moves one atomic jump a previously ordered row may become disordered. Such rows are not of course visible on the electron micrographs. This type of disordering can also occur when the energetic particle is unable to produce cascades.

In all these damage processes point defects are produced and at temperatures where they are mobile, enhanced diffusion occurs. Since ordering is presumed to occur by such point defect motion, the kinetics of the ordering process will also be enhanced. Radiation disordering theory must be able to predict both ordering and disordering rates under irradiation.

Before ordering changes can be described, it is necessary to choose some way to measure the order itself. We choose the long range order parameter of Bragg and Williams,[6]

$$S = \frac{f_{A\alpha} - X_A}{1 - X_A} \tag{1}$$

where $f_{A\alpha}$ is the probability that an A atom will be on a site in the α sublattice and X_A is the fraction of A atoms. This parameter takes no account

of how the disordered atoms are arranged and in particular ignores short range order. Unlike thermal ordering, however, where short range order is critical, most radiation disordering is random. This is because the energetic knock-on atoms have energies larger than the ordering energy and are thus likely to be little influenced by it. However, this ensures that the model will not be applicable to an initially disordered alloy which is likely to develop order by domain nucleation.

2a. Radiation Disordering

If the replaced atoms are exchanged randomly then the disordering rate due to irradiation is obviously dependent upon the instantaneous order

$$\left(\frac{dS}{dt}\right)_{irr} = - \varepsilon K S \qquad (2)$$

ε is the number of replacements per displacement and K is the number of displacements per second. Equation (2) only requires that at long times S should tend to zero.

The fact that in a single set of replacements atoms are not replaced randomly (as in a replacement sequence, for example), does not matter as long as successive sets are randomly spaced, so that no correlation occurs between neighboring sets. Departure from randomness in a single set only changes the magnitude of ε, not the form of the equation. Because Equation 2 is so general, it has been deduced for and found to fit many different irradiation disorder situations.[7,8]

Theoretical values for the replacement ratio ε have varied greatly from ~ 1-1000, and this is a topic of great interest currently from the point of view of cascade studies. The calculation is very difficult requiring

first a determination of the number and size distribution of cascades and then estimates of the replacements and displacements for each size of cascade. For fast neutrons, values of $\varepsilon \gtrsim 100$ seem reasonable while for thermal neutrons values somewhat below this are expected ($\varepsilon \sim 10$). 1 MeV electrons generally give $\varepsilon \sim 1$.

2b. Enhanced Thermal Ordering

Although the thermodynamics of ordering have been heavily studied, the kinetics of ordering have been the subject of very few papers. In a standard paper Dienes[9] used chemical rate theory for a "reaction" in which a pair of wrong or antistructure atoms transform to a right or ordered pair. The result differs from the usual chemical rate result in that increase in the degree of order (extent of reaction) increases the ordering rate. This is, of course, the essence of the ordering reaction as a cooperative process. Dienes demonstrated that if the ordering energy (the energy difference for a wrong and right pair) was taken to be a linear function of the order, the Bragg-Williams result for the equilibrium order was obtained. For the case of Cu_3Au this lies below the experimentally determined values.[10] In the chemical rate approach the rate constant for the ordering reaction is given as

$$k_1 = \nu_1 \exp\ (-U/k_BT)$$

while the reverse disordering reaction rate constant is

$$k_2 = \nu_2 \exp\ [-(U+V)/k_BT]$$

where U is the energy barrier for the pair exchange and V is the ordering energy. ν_1 and ν_2 are the frequency factors which in Bragg-Williams theory are taken to be equal. Dienes obtains

$$\left(\frac{dS}{dt}\right)_{thermal} = \nu \exp(-U/k_BT)\{X_AX_B(1-S)^2 - \exp(-V/k_BT)[S+X_AX_B(1-S)^2]\}$$

where the ordering energy $V=V_oS$.

In order to use this theory to describe the radiation enhanced thermal ordering rate ($dS/dt_{thermal*}$), it is necessary to introduce the point defect concentrations. We first assume:

i) In Cu_3Au interstitial motion does not change the degree of order. The large size difference between the atoms makes this reasonable and it is justified experimentally by the absence of ordering in stage I annealing.[11]

ii) Ordering proceeds by a vacancy mechanism. The increased ordering rates under irradiation are good evidence for this.

The point defect concentrations can be introduced into the rate constants by assuming that the pair exchange occurs by successive vacancy jumps. The energy barrier to pair exchange (U) then becomes the energy barrier to vacancy motion in the double vacancy jump (E_m^o). The frequency is the vacancy attempt frequency divided by two for a double jump. The probability of a vacancy being in position to make the exchange is $(Z_\alpha + Z_\beta - 2)\, C_v$. The term in brackets is the number of sites around the pair, Z_α being the number of α sites around a β site and Z_β the number of β sites around an α site. C_v is the vacancy concentration. The rate constants are then

$$k_1 = (\nu_v/2)\ C_v\ (Z_\alpha + Z_\beta - 2)\ \exp\ (-E_m^o/k_BT) \qquad (3)$$

$$k_2 = (\nu_v/2)\ C_v\ (Z_\alpha + Z_\beta - 2)\ \exp[(E_m^o + v)/k_BT]\ .$$

With these changes we can now write the ordering rate as,

$$\frac{dS}{dt}_{thermal} = (\nu_v/2)\ C_v\ \exp\ (-E_m^o/k_BT)\ \{X_AX_B(1-S)^2 - \exp(-V_oS/k_BT)[S+X_AX_B(1-S)^2]\}. \cdot(Z_\alpha+Z_\beta-2) \qquad (4)$$

As we have noted irradiation increases the vacancy concentration C_v and so enhances dS/dt. To include this effect we use rate theory following Brailsford and Bullough[12] to obtain C_v. The use of this theory implies that the point defects have reached steady-state concentrations, so that using C_{ve} for the equilibrium vacancy concentration,

$$\frac{\partial C_i}{\partial t} = 0 = K_i - D_iC_ik_i^2 - \alpha C_iC_v \qquad (5)$$

$$\frac{\partial C_v}{\partial t} = 0 = K_v - D_vC_vk_v^2 - \alpha C_iC_v + D_vk_v^2C_{ve}$$

$$K_i = K(1-f_i)$$

$$K_v = K(1-f_v)\ .$$

K_i and K_v are the rates of production for the defects which survive both correlated recombination (i.e., immediate recombination of a Frenkel pair) and loop collapse in the cascade. (The f's are the fractional losses to these effects.)

D_i and D_v are the interstitial and vacancy diffusion coefficients, α is the recombination constant[12] while k_i^2 and k_v^2 are the effective sink strengths for interstitials and vacancies, respectively. We consider the case where dislocations are the dominant sinks so that the sink strengths can be written in terms of the dislocation bias factors Z_i and Z_v and the dislocation density ρ_d :

$$k_i^2 = Z_i \rho_d \qquad (6)$$

$$k_v^2 = Z_v \rho_d \quad .$$

Inserting all these parameters, the coupled equations (5) can be solved to give C_v and C_i.

The total vacancy concentration obtained by this solution is:

$$C_v = C_{ve}/2 - Z_i D_i \rho_d/(2\alpha) + \{[C_{ve}/2 + Z_i D_i \rho_d/(2\alpha)]^2 + K_v D_i Z_i/(Z_v D_v \alpha)\}^{1/2} \qquad (7)$$

where the equilibrium vacancy concentration $C_{ve} = \exp(-E_f/k_B T)$.

Note that the vacancy diffusion coefficient is given by $D_v = D_{ov} \exp(-E_m/k_B T)$ in which the average energy for vacancy motion E_m is not necessarily the same as the energy for an ordering jump E_m^o since the vacancy can move over large distances on the copper sub-lattice only. C_v can now be inserted into the ordering equation (4) to give the enhanced ordering rate.

2c. The Order Rate Equation

The actual ordering rate is a balance between the radiation disordering rate of equation (2) and the radiation enhanced ordering rate obtained by inserting the enhanced vacancy concentration of equation (7) into equation (4), giving

$$\frac{dS}{dt} = \frac{dS}{dt}_{irr} + \frac{dS}{dt}_{thermal*} \qquad (8)$$

where the terms on the R.H.S. are obtained from equations (2) and (4).

Results from equation 8 using the parameters of Table 1 are shown in Figure 1. The choice of these particular values will be discussed in the next section. Here certain general features of the results are considered.

Figure 1 shows the variation of dS/dt together with that for its components dS/dt_{irr} and $dS/dt_{thermal*}$. The latter is identical in form to $dS/dt_{thermal}$ obtained by Dienes[9] except for a multiplying factor which contains the enhanced vacancy concentration. This varies with temperature as shown in Fig. 2. At higher temperatures near the order transition temperature the multiplying factor approaches unity as there are so many thermal vacancies that the irradiation increase in their concentration is negligible. Radiation then makes little difference and the thermal ordering rate dominates. At lower temperatures the enhanced ordering rate is the dominant rate as Figure 1 shows. In this region enhanced ordering under irradiation will be observed. If the temperature is lowered still further, although the enhancement in vacancy concentration increases, vacancy mobility decreases and eventually disappears.

Under these conditions the ordering rate is small and the disordering dominates. At a sufficiently low temperature this will always occur. The most interesting temperature region is where radiation ordering and disordering rates have the same magnitude.

It is obvious from the dS/dt curves that no useful information can be obtained from change-of-slope measurements of ordering rates at fixed S values. Figure 3 shows dS/dt for fixed S values plotted against the reciprocal of

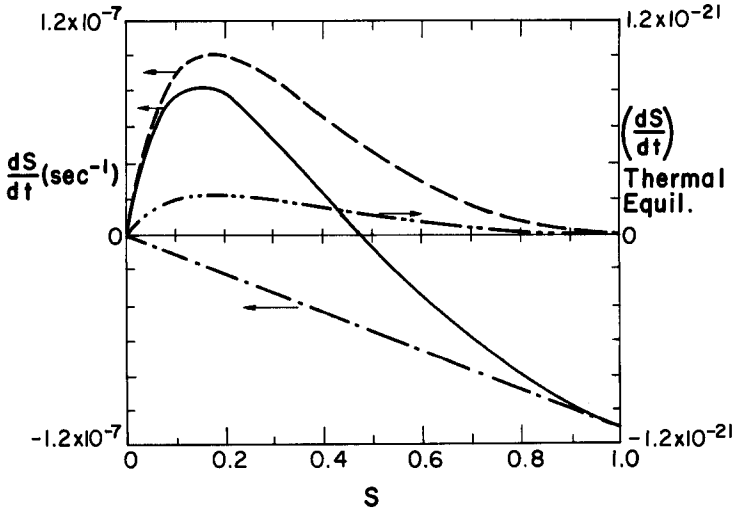

Fig. 1a - The rate of change of order as a function of order parameter S under fast neutron irradiation at 27°C. The irradiation rate was 1.4×10^{-9} dpa/s and ρ_d was $1.7 \times 10^{13}/m^2$.

- . - . - Irradiation disordering rate
- - - - - The irradiation enhanced ordering rate
——— The sum of the above
- .. - .. - The thermal ordering rate in the absence of irradiation, for comparison (note: different scale).

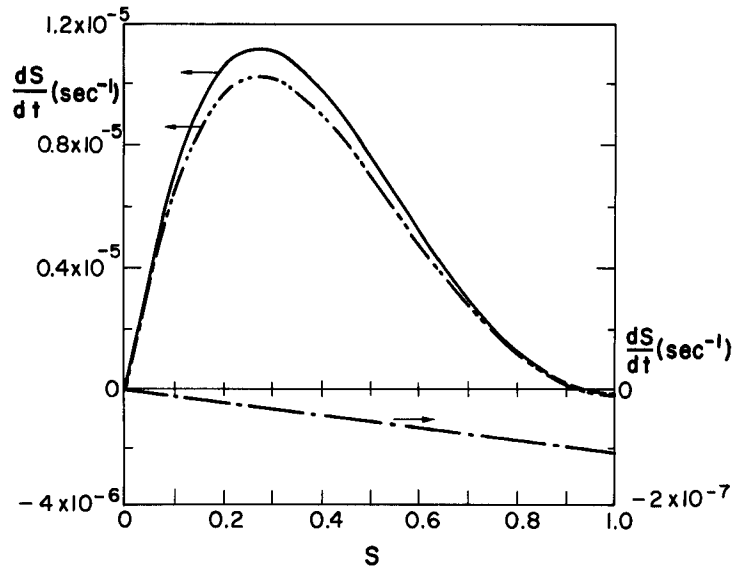

Fig. 1b - As 1a at 302°C. The radiation enhanced ordering curve is so close to the solid line as to be indistinguishable except at high S. (Note different scale for radiation disordering rate.)

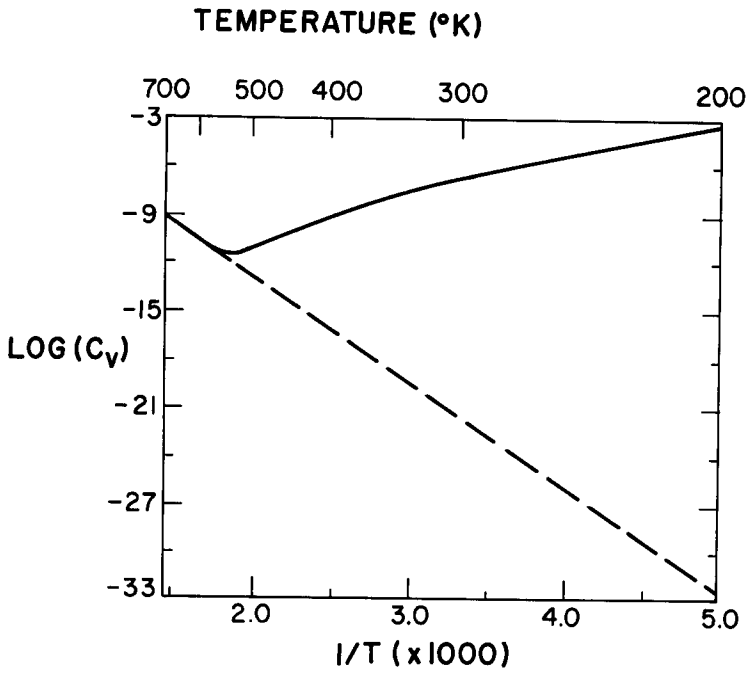

Fig. 2 - The enhanced steady-state vacancy concentration caused by fast neutron irradiation, according to equation (7) versus reciprocal temperature (solid line).

The equilibrium vacancy concentration is shown in the dashed line. The parameters used are those in Table 1 with $\rho_d = 1.7 \times 10^{13}/m^2$ and $K = 1.4 \times 10^{-9}$ dpa/sec.

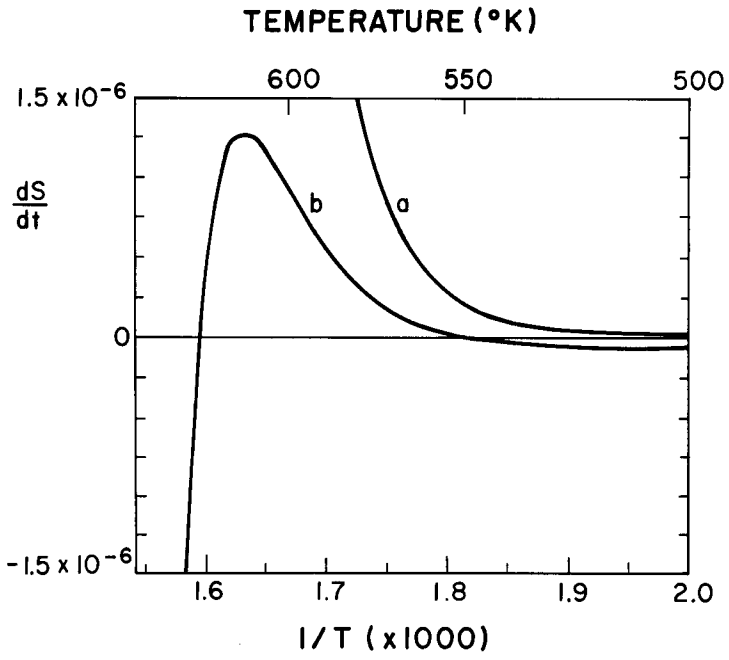

Fig. 3 - The order/disorder rate under fast neutron irradiation as a function of reciprocal temperature for two values of S

(a) S = 0.8

(b) S = 0.87

Note the slope for (b) includes a wide range of positive and negative values making an Arrhenius plot meaningless. The parameters used were $\rho_d = 1.7 \times 10^{13}/m^2$ and $K = 1.4 \times 10^{-9}$ dpa/sec.

Table 1

Parameters Used in Fitting Cu_3Au Data

Vacancy motion energy	$E_m = 0.8$ eV
Vacancy ordering motion energy	$E_m^o = 0.84$ eV
Vacancy pre-exponential diffusion coefficient	$D_{ov} = 7.8 \times 10^{-5}$ m^2/s
Vacancy formation energy	$D_{fv} = 1.28$ eV
Vibrational frequency	$\nu_v = \nu_i = 10^{13}$ Hz
Interstitial motion energy	$E_{im} = 0.12$ eV
Interstitial pre-exponential diffusion coefficient	$D_{oi} = 7.8 \times 10^{-7}$ m^2/s
For fast neutrons	
Vacancy loss fraction	$f_v = 0.95$
Replacement to displacement ratio	$\varepsilon = 80$
For thermal neutrons	
Vacancy loss fraction	$f_v = 0.0$
Replacement to displacement ratio	$\varepsilon = 20$
Dislocation bias for interstitials	$Z_i = 1.02$
for vacancies	$Z_v = 1.0$
Recombination coefficient	$\alpha = 10^{21}/m^2 \times D_i$
Copper concentration	$X_A = 3/4$
Ordering energy	$V_o = 0.35$ eV

temperature. Since dS/dt can be either positive or negative no Arrhenius plot can be meaningful. In fact, the slope of such a plot can vary anywhere from - ∞ to + ∞. Over limited temperature ranges certain values of activation have been extracted[11,14] but the results, as this analysis shows, are meaningless.

Figure 1 also indicates that the ordering and disordering rates balance each other to give dS/dt = 0 over a wide range of S values, depending on temperature. These values of S define a steady-state condition under irradiation where no further change in order takes place. These steady-state values (S_∞) were determined by setting Equation (8) equal to zero and solving numerically. The results are shown as a function of temperature for fast and thermal neutrons in Figure 4a.

The various temperature range effects are clearly visible. At high temperature the thermal equilibrium curve is approached. As the temperature decreases the order remains high due to the enhanced ordering from excess vacancies. As these become immobile at still lower temperatures radiation disordering dominates to give low S_∞ values. It is clear that there is a narrow temperature range over which S_∞ changes very rapidly. This range is itself strongly dependent on the rate and type of irradiation (i.e., upon εK). Fig. 4a shows a plateau in the S_∞ values in the mid-range for the fast neutron case. This arises from the vacancy behavior. At very low temperatures the enhanced vacancy concentration is very large because the immobile vacancies cannot diffuse to sinks and can only be removed by recombination with the interstitials (Fig. 2). However, in spite of this high concentration, the diffusion of matrix atoms remains low because of low vacancy mobility (Fig. 4b). In the intermediate range the matrix diffusion ($D_V C_V$) remains constant with temperature increase because the falling vacancy

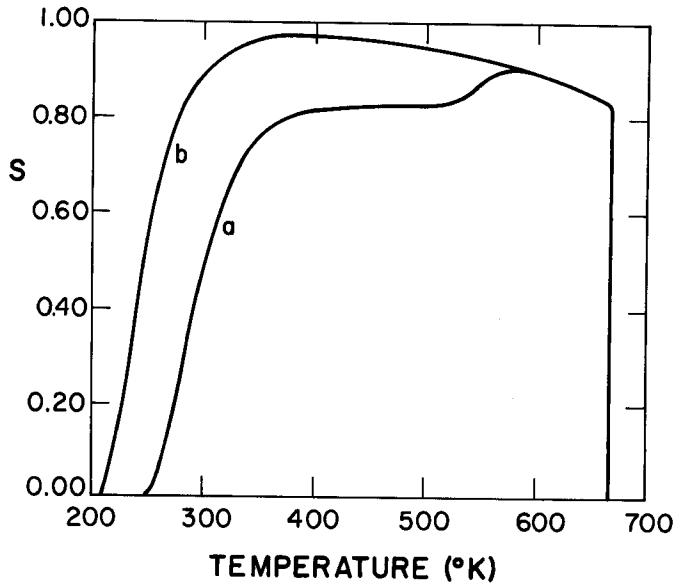

Fig. 4a - The steady-state degree of order, S, as a function of temperature for (a) fast neutrons and (b) thermal neutrons. The parameters are taken from Table 1 with

$\rho_d = 1.7 \times 10^{13}/m^2$ and $K = 1.4 \times 10^{-9}$dpa/s for (a)

$\rho_d = 10^{12}/m^2$ and $K = 2.5 \times 10^{-10}$dpa/s for (b)

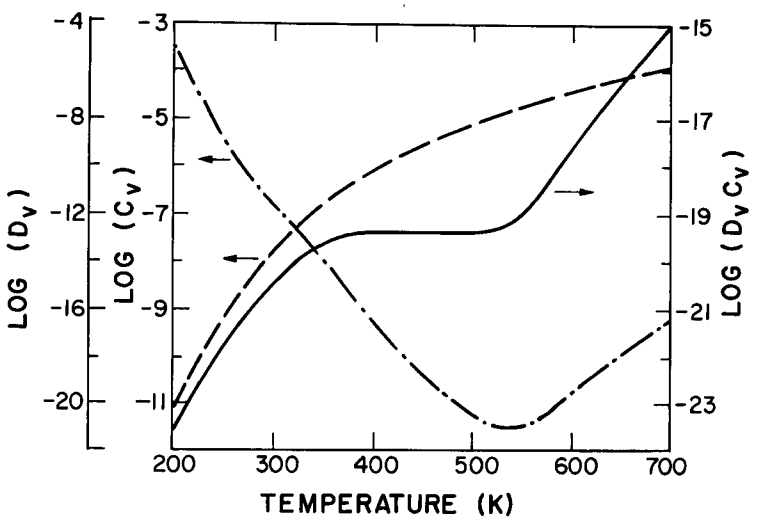

Fig. 4b - The matrix diffusion parameters ($D_V C_V$) for fast neutrons as a function of temperature (solid line). Note the plateau which gives rise to the plateau in Fig. 4a line (a). This arises from the balance between a falling vacancy concentration (dot and dashes) and a rising vacancy diffusion coefficient (dashed line).

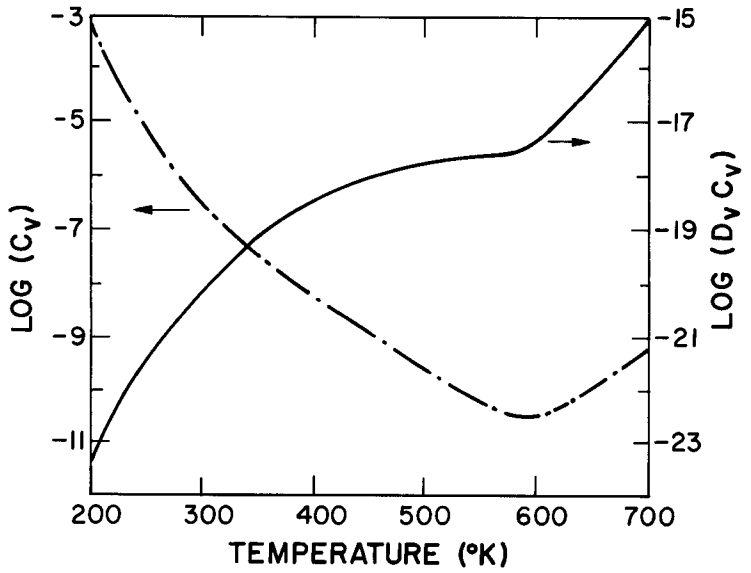

Fig. 4c - As for 4b but for thermal neutrons. Note the absence of a well-defined plateau (even with a logarithmic scale).

concentration is balanced by the increasing mobility (Fig. 4b). The enhanced ordering rate follows the matrix diffusion closely in this range giving a similar shape of the S_∞ curve of Fig. 4a to the diffusion curve in Fig. 4b. At some low value of S_∞ the whole idea of long range order will break down. At this value the alloy will nucleate new ordered domains on reordering, rather than growing back into the original large domains by a gradual increase in S. This critical value of S is not known. (Experiments are not possible by thermal treatment since values of S in Cu_3Au between S=0.8 at T_c and S=0 are unobtainable by this means.)

The rate equation (6) has also been solved numerically for the time dependent case, using $S=S_0$ at t=0 as a boundary condition. The differential equation problem solving package EPISODE[14] was used for this. However, the results were very close to a simple modification of the time dependent analytic solution given in reference 3 (where V_0S now replaces the constant v_0).

$$S(t) = 1-p + \frac{p-q}{1-\left(\frac{S_0+q-1}{S_0+p-1}\right) \exp(zt)} \qquad (9)$$

where $z^2 = \varepsilon^2K^2 + 4 \times [x + \varepsilon K/(1-S_e)]$

$p = (-\varepsilon K+z)(1-S_e)/2x$

$q = (-\varepsilon K-z)(1-S_e)/2x$.

The rate constant x is given by

$$x = \nu C_v (Z_\alpha + Z_\beta - 2)\, Z_\beta [(X_A/X_B)\,(1 - y_e + \Gamma y_e^2)]^{1/2} \qquad (10)$$

$$\cdot [1 + (y_e/2)\,(-V_o/k_BT + \frac{1-2\Gamma y_e}{1-y_e+\Gamma y_e^2})]$$

$$\cdot \exp(-E_m^o/k_BT)\, \exp[(V_o y_e - V_o)/2k_BT]$$

where $y_e = 1 - S_e$ and $\Gamma = X_A X_B$. A typical set of results in the middle temperature range is shown in Figure 5. These curves could be compared directly with experimental results of the order parameter under irradiation.

3. Radiation Disordering Data for Cu_3Au

No experimental values of order parameter determined directly from diffraction experiments on irradiated samples are available in the literature. However, several experiments using electrical resistivity as a measure of order have been reported.

3a. Resistivity and the Order Parameter

There are two theories for the variation of S with electrical resistivity ρ. The first due to Muto[15] (A) gives

$$\rho_S = \Delta\rho\,(1 - S^2) + \rho_{S=1} \qquad (11)$$

(where $\Delta\rho = \rho_{S=0} - \rho_{S=1}$).

The second theory due to Landauer[16] (B) applies to a mixture of two phases and was applied to irradiated and ordered Cu_3Au by Cook and Cushing;[17] it is expressed in conductivity terms:

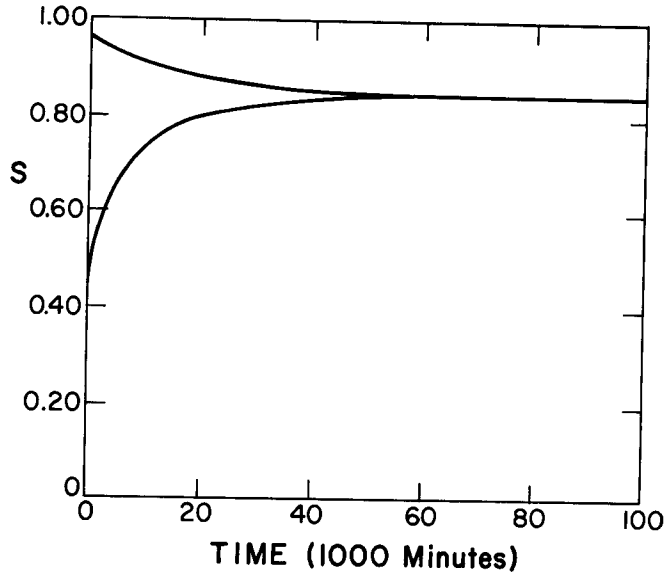

Fig. 5 - A typical set of time dependent results with the parameters of Table 1 and $K = 1.4 \times 10^{-9}$ dpa/sec and $\rho = 1.7 \times 10^{13}/m^2$.

$$\sigma_s = \frac{1}{4}\{(3\chi_2-1)\,\sigma_2 + (3\chi_1-1)\,\sigma_1 + [((3\chi_2-1)\sigma_2 + (3\chi_1-1)\sigma_1)^2 + 8\sigma_1\sigma_2]^{1/2}\} \quad (12)$$

where χ_1 is the fraction of material with conductivity σ_1 and χ_2 similarly with σ_2.

This approach is of doubtful validity in an ordering alloy where disorder involves individual atoms being misplaced. A treatment like that of Muto which treats scattering from individual anti-structure atoms seems more reasonable. In addition to these two theories, Cook and Cushing (C) used a modification of Landauer's model, for which they did not claim high accuracy:

$$\sigma_s = \chi_1\sigma_1 + \chi_2\sigma_2 \ .$$

All three models apply at constant temperature. Since $\rho_{s=1}$ and $\rho_{s=0}$ will have different temperature scattering the temperature coefficients are expected to be different. In addition well ordered Cu_3Au has an anomalous resistivity minimum[19] below about 100°K. Since the various resistivity measurements have been made at a variety of different temperatures, it is first necessary to determine $\rho_{s=1}$ and $\rho_{s=0}$ as functions of temperature. From the data of Passaglia and Love[19] at low temperatures and of Blewitt[18,20] at 0°C and 150°C it is possible to do this (Fig. 6). The resistivity anomaly[19] is clearly shown in the ordered alloy. In the disordered alloy it is much less. Taking these limits for each temperature for which data exists and using the information on the heat treatments it was possible to eliminate models B and C. Blewitt's "partially ordered" sample was quenched from 375°C after a long equilibration. From the experimental equilibrium order curve this should give a value of $S \sim 0.85$. It cannot be less than 0.75 which is the minimum value below T_c. Using the resistivity given by Blewitt of 3.7 μΩm at

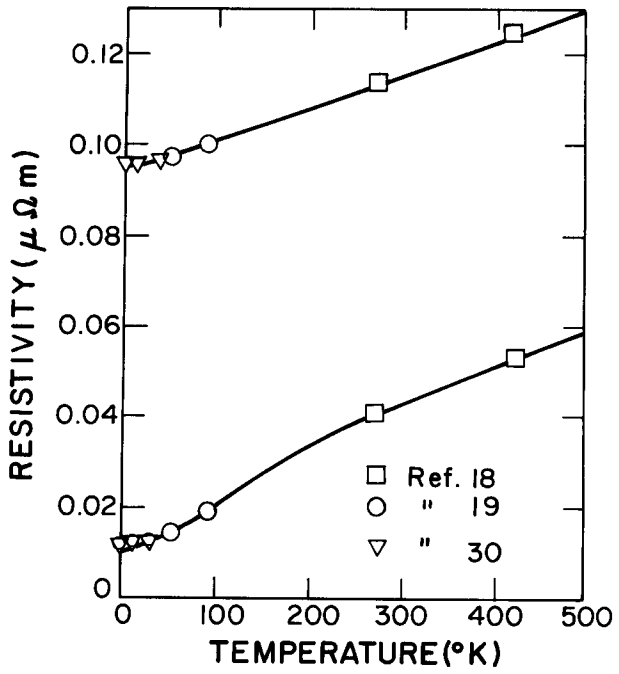

Fig. 6 - The resistivity as a function of temperature for the disordered state, S=0 (upper curve), and the ordered state, S=1.

$4^{o}K$ and 7.7 μΩm at $150^{o}C$ we estimate a value of S=0.83 in good agreement with the equilibrium measurement. Theories B and C gave S=0.39 and S=0.23 respectively. Similar results were obtained for these two theories using other resistivity data; in all cases the S values were far too low. On the other hand, Muto's model (A) gave sensible values for S in the range 0.8-1.0 after long time aging below T_c. In all subsequent analysis, therefore, equation (10) was used together with Figure 6 to determine S from the resistivity reported.

4. Fitting the Experimental Data

As is well known the Bragg-Williams model predicts low values of S when compared with experiment. Since our approach is phenomenological we have chosen to use a value of V_o=0.35 eV which gives a good fit to the equilibrium order parameter S_e as shown in Figure 7. In this way we obtain a correct value for the thermal ordering rate in the absence of irradiation. However, the T_c obtained from this value of V_o by Bragg-Williams equilibrium theory will be larger than the experimental value. We simply cut off the curve at this latter temperature $T_c = 663^{o}K$.

The clearest and most complete data is that of Kirk and Blewitt.[18,20] This includes resistivity versus irradiation time for two S_o values in a predominantly fast neutron flux at $150^{o}C$ and $4^{o}K$, and one S_o value for a primarily thermal neutron flux at $135^{o}C$. These are shown in Figure 8 with the theoretical curves fitted from our theory.

The $4^{o}K$ data (Fig. 8a) are fitted with the disordering rate only (Equation 2). The only variation in these two curves is due to differing S_o and this is fixed from the resistivity data. Both curves must have the same value of εK, so these data offer a severe test of the disordering model. Agreement is satisfactory, the small deviations probably being due to small deviations from a quadratic resistivity dependence on S.

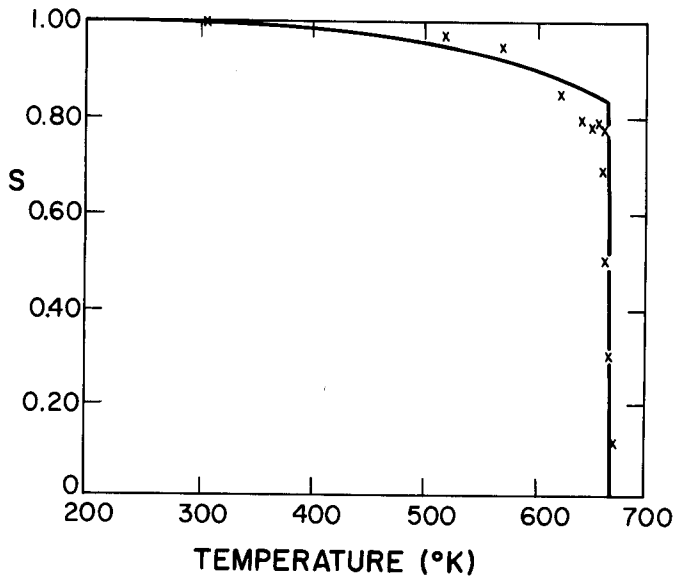

Fig. 7 - The thermal equilibrium order curve as a function of temperature (V_o = 0.35 eV). The experimental data are from Keating and Warren.[21]

To separate ε and K we need an independent estimate of the displacement rate K. This has been discussed by Kirk and Blewitt[18] in their own analysis of their data.

Using primary displacement cross sections of 3 barns and 5.5 barns for copper and gold, respectively, and displacement thresholds of 25 eV and 45 eV, the fast neutron irradiation rate of 2×10^{16} neutrons/m^2/sec gives a displacement rate of 1.4×10^{-9} dpa/sec. For the εK values taken from Fig. 8a this gives $\varepsilon = 80$.

With these values of εK the high temperature data can now be fitted. However, since no electron microscopy analysis of dislocation density is available we have no information with which to model how ρ_d varies with time. We, therefore, used constant values for this parameter. (There is no difficulty in accommodating a changing ρ_d in our model once such data becomes available.) Since most of the data covers only the early stages of irradiation (total dpa $\lesssim$ 0.01) and relatively low temperatures we anticipate that recombination will dominate early in the process when ρ_d is low but that intermediate values of ρ_d (10^{12} - $10^{16}/m^2$) will become influential later. The pre-exponents in the diffusion coefficients D_{ov} and D_{oi} and the interstitial motion energy E_{im} were all taken from copper data.[22]

The vacancy motion energy was taken from the Cu_3Au literature[23-25] to lie in the range 0.8-1.1 eV. The energy of motion for an ordering jump was chosen to be slightly larger than E_m.

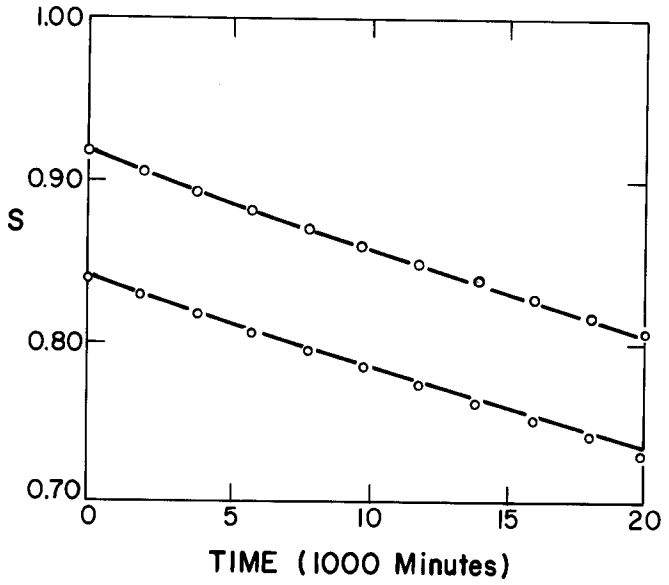

Fig. 8a - The change of order during fast neutron irradiation of Cu_3Au at 4°K from Kirk and Blewitt[18] (points). The two curves represent different starting values of the order parameter. The lines represent a data fit using the parameter values in Table 1 with $K = 1.4 \times 10^{-9}$ dpa/sec and $\varepsilon = 80$.

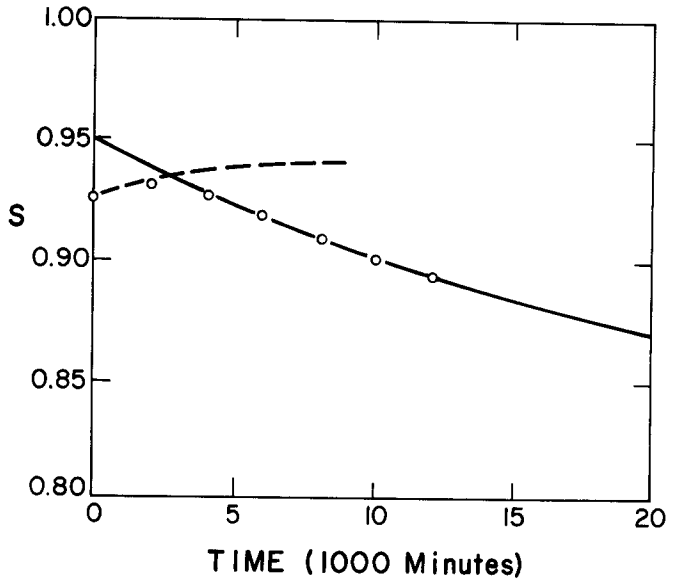

Fig. 8b - The change of order during fast neutron radiation of Cu_3Au at 150°C from Kirk and Blewitt[18] (points). The line represents the fit to the data using the ε and K from Fig. 8a and $\rho_d = 1.7 \times 10^{13}/m^2$. Note the initial transient where the datum points deviate from the curve. For low dislocation densities the vacancies are removed primarily by recombination (dashed line). Under this assumption the initial transient can be fitted.

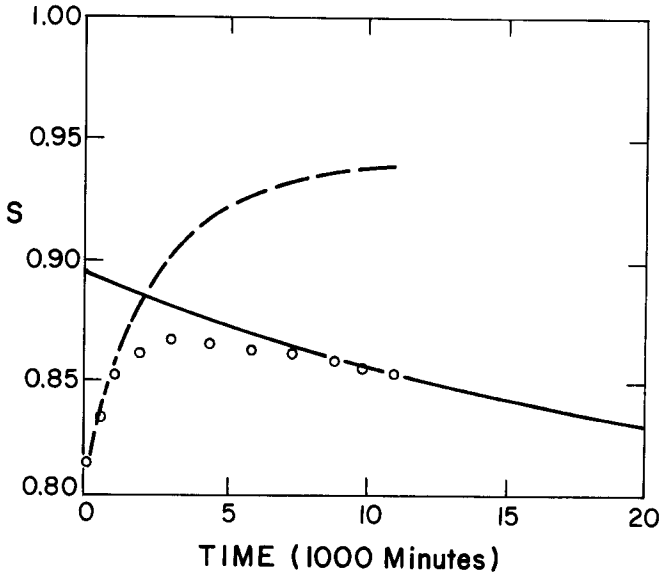

Fig. 8c - As Fig. 8b but for a lower initial order parameter and $\rho_d = 2.7 \times 10^{13}/m^2$ (solid line). Note again the recombination dominated curve (dashed line) fitting the initial slope.

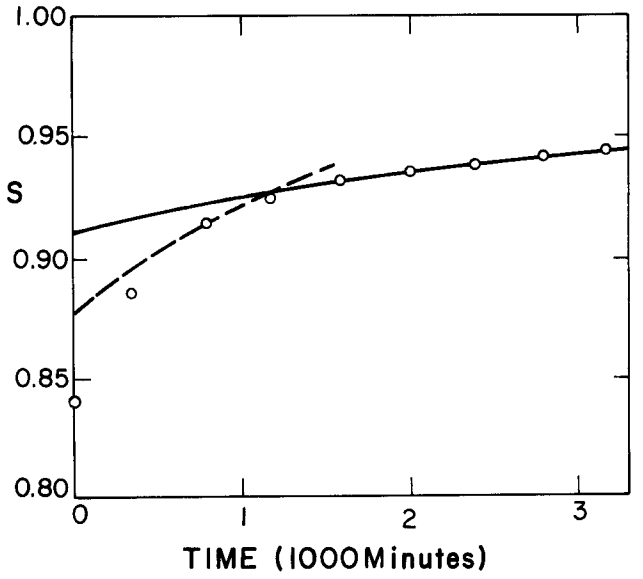

Fig. 8d - As for Fig. 8b but for thermal neutron irradiation[18] at 135°C with ε = 20, K = 2.5 x 10^{-10}dpa/sec and ρ_d = $10^{12}/m^2$ (solid line). Note the recombination dominated curve (dashed line) only explains part of the transient.

Determination of C_v also requires evaluation of the cascade loss fractions f_i and f_v for interstitials and vacancies, respectively. These are not well known but have been discussed by Wollenberger[26] who presents data supporting a value of $f_v = 0.7$ for copper under fast neutrons at low temperature (55-140°K). Kirk and Blewitt suggested a value of 0.95 from their experiment at 150°C. We take this latter value for f_v and f_i. The results are not sensitive to small changes in these parameters.

Figure 8b shows that using these parameters gives an excellent fit to Kirk and Blewitt's data after an initial transient was complete. These workers suggested that the transient may be due to very long free vacancy lifetimes in the early stages when the dislocation density was very low. Under such conditions the vacancy concentration is controlled by the rate of recombination with interstitials. Fig. 8b demonstrates that by using a zero dislocation density the initial slope of the transient can be fitted. The vacancy lifetime under these conditions is ~ 250 s compared with the ~ 2 s for the steady-state with a dislocation density of $2 \times 10^{13}/m^2$. Thus, although the same number of vacancies are produced in each case, the vacancy concentration and hence the ordering rate is much greater for the low dislocation situation.

The dislocations do not become a significant sink until ρ_d reaches $\sim 10^{11}/m^2$ so that similar curves are obtained to the one shown in Fig. 8b (dashed line), up to this dislocation density.

The length of the transient is a measure of the time needed for the dislocations to dominate as sinks. It is clear that ρ_d is changing much more slowly than the order parameter. (This is why one can speak meaningfully of a steady-state order even when the dislocation density is varying.) In fact, the dislocation density will steadily increase[29]

and saturate after several dpa. In contrast order steady-state is reached after ~ 0.01 dpa. This implies that our so-called steady-state order will change somewhat with the dislocation density, tending to drift slowly lower with very long irradiation times.

This suggestion for the transient also explains why it has a larger magnitude for specimens with lower order (Fig. 8b). In such specimens the vacancies during their extended lifetime at the beginning of reaction meet more wrong atoms than in more highly ordered samples. All this is automatically accounted for in the model.

For the thermal neutron flux no low temperature data was available so that εK was chosen to fit the experimental data. The other parameters, however, are fixed from the fast neutron fit and were not changed. The curve was fitted successfully as shown in Figure 7c, by using $\varepsilon = 20$ and $K = 2.5 \times 10^{-10}$ dpa/s. Taking cross sections for the (n,γ) reaction of 98 barns and 4.4 barns for gold and copper, respectively, and a given flux of 2×10^{16} neutrons/m^2/sec, we obtain $K \sim 10^{-10}$ dpa/s in reasonable agreement with our fitting parameter.

Note that in this case we have very small cascades, the component defects of which may be well separated if a replacement collision sequence occurs. To fit the data we required a vacancy survival rate of 100%, indicating that such sequences are quite common.

With the aid of our fitted line it is now clear that this data contains a transient also, no doubt for the same reason as before. Fig. 8c includes the low dislocation density result which in this case only explains part of the transient. A closer fit could be obtained by using a smaller value

for ε and a correspondingly higher K. However, this would deviate from the calculated K and the ε value determined by Kirk and Blewitt.[18] If these values are reliable the results suggest that a further explanation is required for the remaining transient for thermal neutrons.

The predominance of long replacement collision sequences (implied by the high vacancy survival rate) for thermal neutrons indicates that the disorder in the early stages consists primarily of such sequences. Since each faulted row can be easily ordered by one vacancy moving along it, it is probable that the ordering rate will be increased initially, until overlap of sequences occurs. This is the probable explanation of the remaining transient.

In the fast neutron case where most replacements occur in the cascade, the disordered region is three-dimensional. Only the wrong atoms on the outermost layer of the disordered region are adjacent to the matrix which is defining the long range order of the sites. Only in this outer layer will vacancies be able to re-order with anything like the high efficiency of vacancies moving along replacement collision sequence traces. Since our simple model makes no allowance for such differences in the distributions of wrong atoms there will be part of the transient that cannot be fitted in the thermal neutron (high vacancy efficiency) case. As radiation proceeds overlap of collision sequences will increase the three-dimensional nature of disordered regions. The ordering effectiveness of vacancies will then approach the fast neutron case.

The remaining data for irradiation of Cu_3Au in the literature is much older and reactor dosimetry was less complete. Sufficient details of the nature and magnitude of the fluxes are, therefore, lacking. However,

we were able to fit all these data successfully with our model using the same defect parameters established above. The only parameters changed were ρ_d and K.

Figure 9 shows our fit to the data of Cook and Cushing.[17] It is important that the values of E_m and E_m^o give the correct temperature variation since this data is taken at a temperature 100°C below that of Kirk and Blewitt.[18] The irradiation rate used by Cook and Cushing was estimated at 4×10^{16} neutrons/m^2/sec (3×10^{-9} dpa/s). These workers observed similar resistivity curves at 106°C and 35°C. These translate to the different order curves shown in Figure 9.

These curves were successfully fitted with the identical diffusional parameters to those in Fig. 8b, indicating that E_m and E_m^o correctly predict the temperature variation from 35°C-150°C. These data extend to twelve times the dpa of the data in Fig. 8b. It is, therefore, not surprising that we find a higher dislocation density necessary to fit the curve. No transient is visible in these curves, presumably due to the lower temperature.

Figure 10 shows our fits to the thermal neutron data of Glick, et al.[27] and fast neutron data of Siegel.[28] We emphasize that once again the only parameter changes involve ρ_d and K which take the values shown in the figure. Once again a very satisfactory fit is obtained.

In Figure 10a, the data of Glick[27] during irradiation of an initially ordered and an initially disordered sample with thermal neutrons are shown. The ordered data can be fitted accurately with the same diffusional parameters as before. For the initially disordered sample, the data can be fitted except

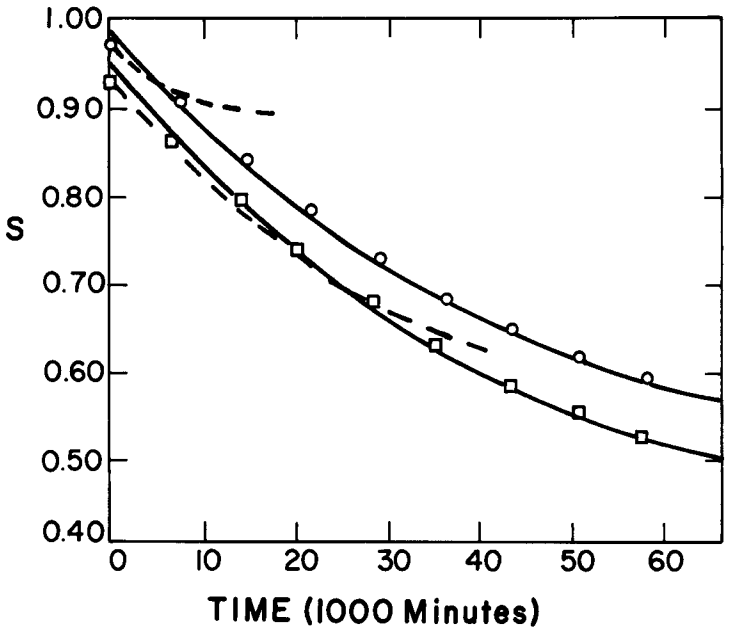

Fig. 9 - The data of Cook and Cushing[17] for fast neutron irradiation at 35°C and 106°C. The points are fitted with the curves shown using $K = 3 \times 10^{-9}$ dpa/sec and $\rho_d = 2.5 \times 10^{14}/m^2$ at 106°C (upper curve) and 35°C (lower curve).

for the initial transient. The explanation for the transient is presumably similar to that given in the discussion for thermal neutron data above (Fig. 8c). However, the very low value of S probably means that a small domain size exists in the sample and a short range order model should really be used for the data.

Finally, Fig. 10b shows the fitting to the fast neutron data of Siegel[28]. Once again, the same diffusional parameters are used, indicating that the E_m and E_m^o values correctly predict the temperature variation.

Figures 8-10 contain only very small initial transients as compared to Fig. 7. The former were for data at a much lower temperature however. This has little effect on interstitial mobility so that vacancy lifetime is not affected much. (Vacancies are effectively stationary compared with interstitials at all these temperatures.) On the other hand, since the vacancy jump frequency is greatly reduced at the lower temperatures, the number of ordering jumps made by a vacancy is greatly reduced at the lower temperatures. As Figures 8-10 show the resulting differences between the curve for recombination only and the curve for higher dislocation density are much closer than in Fig. 7. As vacancies become less mobile at lower temperatures, recombination becomes more important than flow to dislocations even for high dislocation densities. The initial transients then become negligible.

5. Discussion

The successful fitting of such a varied collection of data with similar parameters in a straightforward phenomenological model is remarkable. It should not be thought that this is because the curves can be fitted with a

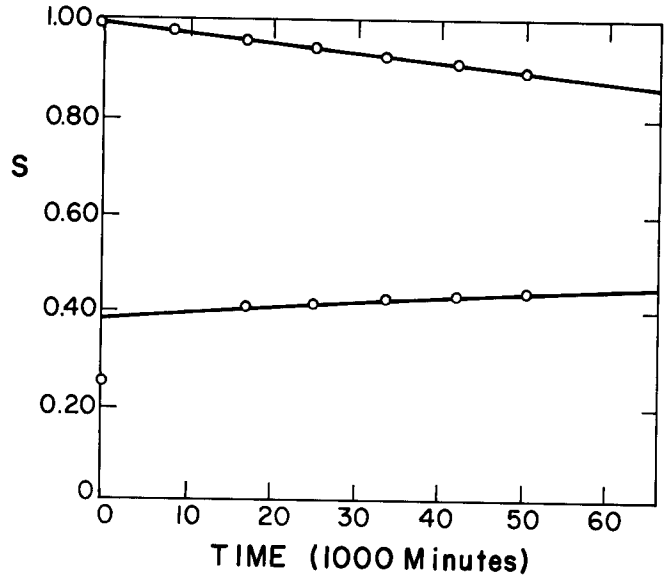

Fig. 10a - Order-disorder change under thermal neutron irradiation at 80°C measured by Glick et al.[27] fitted using $K = 2 \times 10^{-9}$ dpa/sec and $\rho_d = 1.5 \times 10^{16}/m^2$. Note the very low value of S for the low curve.

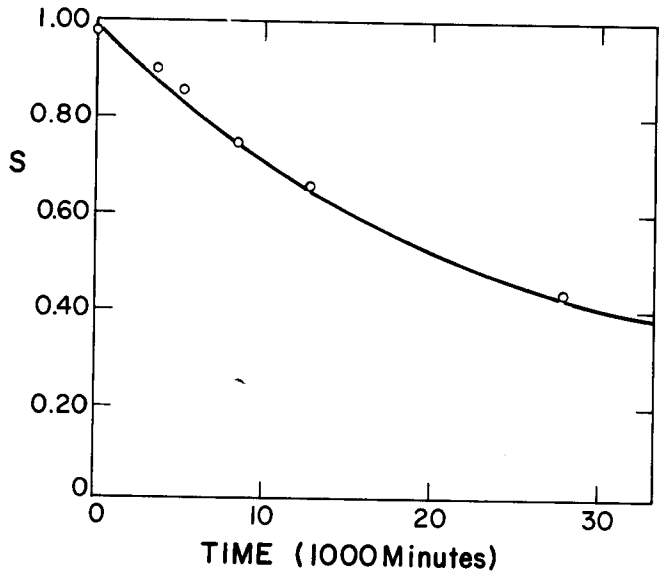

Fig. 10b - The fast neutron data of Siegel[28] at 40°C, fitted using $K = 8 \times 10^{-9}$ and $\rho_d = 8 \times 10^{14}/m^2$.

wide range of different parameter combinations. In fact the choice of the key parameters is very narrowly restricted.

The ordering energy V_o is fixed by the requirement of matching the thermal equilibrium order at low and intermediate temperatures. The multiple εK is fixed by the low temperature experiments. The diffusional parameters are not well known (D_{ov}, D_{oi}, E_{im}, E_v^o, E_{vf}, ν). The interstitial diffusion however must be rapid at these temperatures which implies that the exact value of motion energy E_{im} is less important than the fact that it is small. D_{ov} and ν can be adjusted to compensate for a change in vacancy motion energy E_m and hence it is possible to match the same data at a given temperature with various combinations. However, it is impossible to match the data at <u>different</u> temperatures in this way. In fact the strong temperature variation very closely limits the values of E_m and E_m^o to those given in Table 1. However, it is possible to decrease E_m and simultaneously increase E_m^o in such a way that the quality of fit only decreases slowly. From the current data therefore we can only fix their combination precisely. The current values are accurate to ±0.05 eV, but the combination is better than that. However, with more data at steady-state it should be possible to fix these energies very precisely since the shape of the predicted S_∞ versus temperature curve varies strongly with such changes. Since the same parameters used for the time dependent curves were used to determine the steady-state order curves of Fig. 4, we believe that the latter give an accurate prediction. The only remaining variation is the slow change in the dislocation density as radiation proceeds. The next step in our theory will model such a changing dislocation density and its effects.

From the point of view of our model the current data is very incomplete. An ideal experiment would be to irradiate Cu_3Au for longer times at a wide range of temperatures. Each flux should also be used at low temperatures (below room temperature) to determine εK. It is essential that all experiments begin with large domain size and a well defined order parameter. The dislocation density variation should be monitored also. With this information our model could be tested much more completely. The results so far suggest that these experiments could provide accurate data for point defect behavior in Cu_3Au and detailed information on cascades as a function of temperature.

There is an urgent need for an experimental test of Muto's[15] model relating resistivity and the long range order parameter.

We note also that radiation is a very useful tool in the study of order/disorder reactions. The enhanced ordering rate could well be used to produce more completely ordered materials at lower temperatures where the thermal reaction is too slow to go to completion. In addition, lower values of S can be obtained by low temperature irradiations than can be obtained by thermal treatments. This will permit the study of ordered alloys over a much wider range of S than has been used hitherto.

6. Conclusions

a) The radiation disorder model has been shown to successfully fit all available long time data for fast and thermal neutron irradiations.

b) The parameters critical to the fitting are:

E_m = 0.8 eV for vacancy motion

E_m^o = 0.84 eV for ordering vacancy jumps.

The ratio of replacements to displacements $\epsilon = 80$ for fast neutrons and 20 for thermal neutrons. For the former a survival rate for free vacancy production is 5%, for the latter it is 100%.

c) Initial transients occur in which the ordering rate is much greater. These are explained by the longer lifetime for vacancies at early times when recombination alone controls the vacancy concentration.

d) Predictions for steady-state conditions have been made and their variation has been shown to be physically reasonable.

e) Interpretations of experiments which measure ordering rates and obtain activation energies directly from them are not reliable and this model should be used instead.

Acknowledgements

We are grateful for helpful discussions of this work with Dr. M. Guinan of Lawrence Livermore Laboratory and Drs. T. Blewitt and M. A. Kirk from Argonne National Laboratory. One of us (PW) is grateful for support from the Office of Fusion Energy, U. S. Department of Energy through Lawrence Livermore Laboratory which enabled some of the computational work to proceed.

References

1. K. R. Russell, Jnl. Nuclear Matls. 83, 176 (1979).
2. P. Wilkes, Jnl. Nuclear Matls. 83, 166 (1979).
3. K-Y. Liou and P. Wilkes, Jnl. Nuclear Matls. (in press).
4. E. M. Schulson, Jnl. Nuclear Matls. 83, 239 (1979).
5. M. L. Jenkins, M. Wilkens, Phil. Mag. 34, 1155 (1976).
6. W. L. Bragg and E. J. Williams, Proc. Roy. Soc. A145, 699 (1934).
7. L. R. Aronin, Effect of Nuclear Radiation on the Structure and Properties of Metals and Alloys.
8. V. S. Polenok, Fiz. Met. Metalloved 36, 195 (1973).
9. G. J. Dienes, Acta Met. 3, 549 (1955).
10. D. R. Chipman, Jnl. Appl. Phys. 27. P739 (1956).
11. J. Gilbert, H. Herman, A. C. Damask, Rad. Eff. Vol. 20, (1973), P37.
12. A. Brailsford, R. Bullough, Jnl. Nuclear Matls. 44, 121 (1972).
13. G. Oleownik, W. Schule, Fundamental Aspects of Radiation Damage in Metals, Vol. 1, NTIS, U. S. Department of Commerce, Springfield, VA (1975), P341.
14. A. C. Hindmarsh, J. D. Byrne, Numerical Methods for Differential Systems, L. Lapidus and W. E. Scheisser, eds., Academic Press (1976), 147.
15. R. Muto, Inst. Phys. Chem. Res. Sci. Paper (Tokyo), 20, 99 (1936).
16. R. Landauer, Jnl. Appl. Phys. 23, 779 (1952).
17. L. G. Cook and R. L. Cushing, Acta Met. 1, 539 (1953).
18. M. A. Kirk and T. H. Blewitt, Met. Trans. 9A, 1729 (1978).
19. E. Passaglia, W. F. Love, Phys. Rev. 98, 1006, (1955).
20. T. H. Blewitt, private communication.
21. D. T. Keating and B. E. Warren, Jnl. App. Phys. 22, 286 (1951).
22. N. L. Peterson, Jnl. Nuclear Matls. 69 & 70, 3 (1978).

23. S. Takamura, S. Okuda, Rad. Effects 17, 151 (1973).

24. R. Feder, M. Mooney, A. S. Nowick, Acta Met. 6, 266 (1958).

25. R. A. Dugdale, Phil. Mag. 1, 537 (1956).

26. H. Wollenberger, U. Thesis, to be published in Jnl. of Nucl. Matls.

27. H. Glick, F. C. Brooks, W. F. Witzig, and W. E. Johnson, Phys. Rev. 87, 1074 (1952).

28. S. Seigel, Phys. Rev. 75, 1823 (1949).

29. W. G. Wolfer, Int. Conf. on Fundamental Mechanisms of Radiation Induced Creep and Growth, Chalk River, Canada (1979).